Kinetics of aggregation of carbon clusters

J. Bernholc

*Corporate Research Science Laboratories, Exxon Research and Engineering Company,
Annandale, New Jersey 08801*

J. C. Phillips

AT&T Bell Laboratories, Murray Hill, New Jersey 07974

Gas-phase cluster aggregation is simulated by a model which includes the simultaneous growth of neutral and charged clusters in a laser vaporization source. Electronic-structure calculations determine the kinetic parameters of the model. Results for carbon clusters are in good agreement with experimental data, explain the magic numbers in the C_{10}–C_{25} region, and demonstrate the importance of both thermodynamic and kinetic effects on the cluster growth process.

In the past few years it has become possible to study the gas-phase aggregation of clusters.[1] Most of the work has concentrated on materials with a low boiling point, but the advent of the laser vaporization source[2-4] has allowed for studies of cluster formation of strongly bonded materials, like semiconductors or refractory metals. We have developed a kinetic model of cluster formation which simulates cluster growth in a beam starting from the atomic vapor. Both monomer addition and cluster-cluster aggregation are allowed. Geometrical information and electronic structure calculations are used as input in order to determine the relative cluster-cluster sticking probabilities. Time-dependent coagulation frequencies depend on both these probabilities and on the concentrations of the reacting species.

The primary results of the supersonic beam experiments are spectra of the relative abundance of clusters as a function of the mass of the cluster. These spectra often show relative maxima at particular sizes of the clusters, the so-called magic numbers. By interpreting the magic clusters as more stable thermodynamically than their neighbors, one has been able to infer the geometrical structures of the magic clusters. The analysis of the formation of rare-gas clusters, where magic clusters up to 1000 atoms have been interpreted,[5] and of alkali-metal clusters,[6] provide successful examples of this approach.

For covalently bonded materials, the directional nature of the bonding places severe constraints[7] on the atomic arrangement in the cluster. These constraints are different for carbon, which often forms multiple bonds, and silicon and germanium, which in general do not. It is therefore not surprising that the carbon spectrum[3,8,9] is very different from the silicon[4,9] or germanium spectra.[10] The structural models of larger silicon clusters may involve fragments of the crystalline silicon network,[11] although the dangling-bond-driven relaxation is relatively large.[12] In contrast, the carbon clusters discussed below are purely molecular in nature.

The carbon spectra of Fürstenau and Hillenkamp,[8] of Rohlfing, Cox, and Kaldor,[3] and of Bloomfield, Geusic, Freeman, and Brown[9] are shown in Figs. 1(a)–1(c). The spectra in Fig. 1(a) were obtained by laser vaporization of a thin carbon foil in vacuum, while the remaining spectra involved both laser vaporization and expansion in the pres-

ence of a carrier gas. The label $C_n \rightarrow C_n^+$ denotes data obtained by photoionization of neutral clusters and subsequent detection in a mass analyzer, while the C_n^+- and C_n^--labeled data are of charged clusters produced directly in the beam by aggregation of charged and neutral particles following a strong laser vaporization pulse.

We have studied clusters in the C_1–C_{25} range. In this range the experimental results show numerous magic numbers, several of which are the same under very different experimental conditions. In particular, all three sets of experiments give identical magic numbers for the positively charged clusters in the C_{10}–C_{25} range, and there is a good but not perfect correspondence between the magic
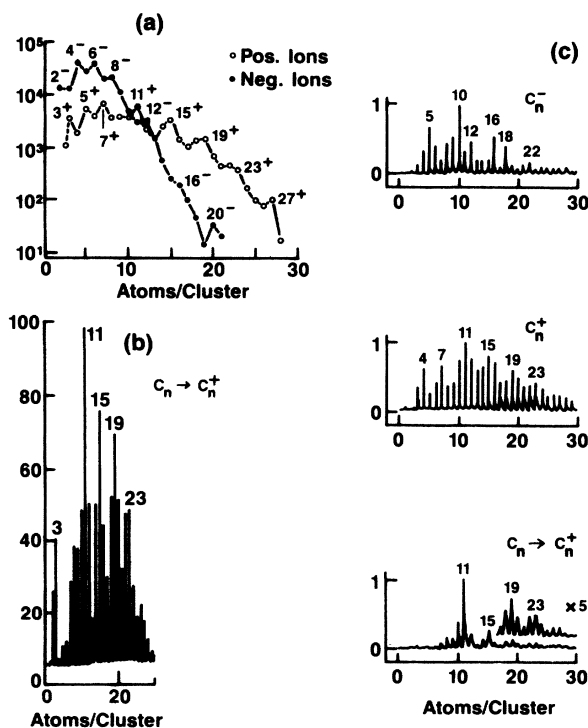
FIG. 1. Experimental abundance spectra of carbon clusters (a) from Ref. 8, (b) from Ref. 3, and (c) from Ref. 9.

numbers for negative clusters in the same range [cf. Figs. 1(a) and 1(c)].

The magic numbers of the positively charged clusters show a $4n + 3$ periodicity in the $C_{10}-C_{25}$ range [Figs. 1(a)-1(c)]. This periodicity is reminiscent of Hückel's rule,[13] which states that a hydrocarbon containing $4n + 2$ π electrons is aromatic and particularly stable, e.g., benzene. Pitzer and co-workers[14] have developed a simple empirical model of π electrons in neutral carbon chains and even-numbered rings. According to their model, neutral C_2-C_9 clusters form π-bonded chains with the odd ones being the most stable. A transition to neutral π-bonded rings should occur around C_{10}. The fourfold periodicity in the rings has the same origin as in Hückel's rule, the π orbitals for the pure carbon rings being both in plane and perpendicular to the plane of the ring, and each carbon atom contributing two π electrons.

We have carried out self-consistent modified neglect of differential overlap (MNDO) calculations[15] for neutral, positive, and negative chains and rings in the C_1-C_{26} range.[16] These structures were chosen because of the well-known tendency of covalently bonded species to minimize the number of dangling bonds. More complicated structures with an increased number of dangling bonds are not favorable energetically for small clusters, since the difference between a σ and a π bond is only about 20 kcal/mole. A ring does not have dangling bonds, but the strain associated with bending sp bonds makes this structure favorable only for larger clusters (see below). In addition to chains and rings, the configurations corresponding to the structures of naphthalene ($\underset{\sim}{1}$) and anthracene ($\underset{\sim}{2}$)

$\underset{\sim}{\mathbf{1}}$ $\qquad\qquad$ $\underset{\sim}{\mathbf{2}}$
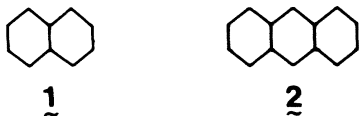
have been geometry optimized and found to have formation energies 130–250 kcal/mole greater than the monocyclic rings. This is due to the greater strain energies in the six-membered rings.

The formation energies per atom ΔH_n for the lowest-energy neutral structures are shown in Fig. 2(a). Note the aromatic minima at 10, 14, 18, and around 22. In Figs. 2(b)-(d) we show the scaled derivative

$$\Delta H_n' = n(\Delta H_{n+1} - \Delta H_n) \ , \tag{1}$$

for neutral, positive, and negative clusters. The peaks in $\Delta H_n'$ correspond to the structures locally most stable against atom addition. Note also the significant charge-induced differences in the relative cluster stability. The structure in $\Delta H_n'$ below C_{10} disappears in the charged species, and there are shifts and/or sharpening of the positions of the peaks at and above C_{10}. For example, the most stable large neutral clusters are C_{10}, C_{14}, C_{15}, C_{18}, C_{19}, and C_{23}; the most stable positive ions are C_{11}^+, C_{15}^+, C_{19}^+, and C_{23}^+; and the most stable negative ions are C_{14}^-, C_{18}^-, and C_{22}^-.

In the kinetic calculations we make the mean-field approximation and solve the Smoluchowski equations[17]

$$dx_i/dt = \sum_{j=1}^{i-1} K_{j,i-j} x_j x_{i-j} - \sum_{j=1}^{N} 2K_{ij} x_i x_j \ , \tag{2}$$

where x_i are the relative concentrations of clusters with i
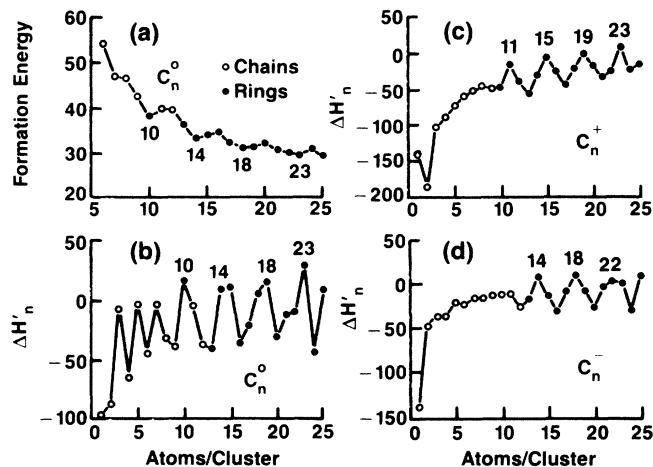
FIG. 2. (a) Formation energy per atom in kcal/mole for neutral clusters, (b)-(d) relative cluster stability of neutral, positively charged, and negatively charged clusters. See text.

atoms, and the kernel K_{ij} represents the probability of the aggregation of clusters i and j to form cluster $i + j$. Equation (2) has been generalized to include the growth of positively and negatively charged clusters via neutral-positive and neutral-negative cluster aggregation.

During the growth process there is also a relatively large probability for a charge-transfer reaction involving a transfer of an electron from a negative cluster to a neutral cluster without aggregation of the two clusters.[18] We have included terms corresponding to this process into the rate equations.

The general shape of the cluster distribution and the high abundance of small carbon clusters show that monatomic vapor is the dominant product of laser vaporization, although a small number of much larger particles can also evaporate from the target. Kroto et al.[19] argue that clusters around C_{60} have been formed from such fragments. Since the fragments are large and their concentration small compared to that of the smaller clusters (see Ref. 9), the presence of fragments would not significantly affect the growth of clusters in the C_2-C_{25} range. The calculations were thus started with the initial conditions corresponding to a weakly ionized monatomic vapor. The degree of ionization was determined from the boiling temperature of carbon and a vapor pressure of several atmospheres. The results are not dependent on these conditions as long as the degree of ionization remains very small.[20]

The major task is the determination of the aggregation and charge-transfer kernels. The aggregation kernel for the neutral clusters is taken to be

$$K_{ij} = \alpha \exp[-\gamma(\Delta G_i' + \Delta G_j')/kT] , \tag{3}$$

where $\Delta G_i'$ denotes the scaled derivative of the Gibbs free energy defined in analogy to Eq. (1), and α and γ are adjustable parameters. The parameter α accounts for initial cluster concentration. The expression in the exponent assumes that the first step of the reaction proceeds via a transition state involving an interaction between primarily two atoms, one on each of the two reacting clusters. The lowering of transition-state free energy is taken to be proportional to the exothermicity of this step[21] with the proportionality factor γ. The form (3) of the kernel is valid in the

reaction-limited regime,[22] as opposed to the diffusion-limited regime of the usual aggregation kinetics. The influence of steric factors on the reaction rate is neglected.

The expressions for the neutral-positive and neutral-negative aggregation kernels are analogous to Eq. (3), with $\Delta G_j'$ replaced by the one corresponding to the charged specie. The same values for the parameters α and γ were used for all three kernels.

The charge-transfer kernel was approximated similarly, with the lowering of the activation energy taken proportional to the difference in electron affinities, with the proportionality constant ξ. The electron affinities were calculated as total energy differences between the neutral and negatively charged species.

The clusters are assumed to be in their lowest energy configurations, since the energy released in fusion allows for structural rearrangements for cluster sizes under consideration. The empirical entropy values are taken from Ref. 14. Since the entropy of rings is lower than that of chains, the equilibrium structure (i.e., chain or ring) at and above C_{10} depends on the effective growth temperature. The solutions of the coupled kinetic equations for the neutral, positive, and negative clusters are shown in Figs. 3(a)–3(c). The average growth temperature and the parameters α, γ, and ξ were adjusted to give the best relative fit for the positive ions in the $C_{10}{}^+$–$C_{20}{}^+$ region, because in this region all experiments produced the same magic numbers. A good fit around $C_{11}{}^+$ with the entropies from Ref. 14 required $T \leqslant 500$ K, showing that the cooling by the carrier gas is very efficient[23] (this temperature is a sensitive function of the entropy difference between chains and rings). At 500 K the structures of the clusters are the same as in Fig. 3, the only exceptions being $C_{10}{}^+$ and $C_{12}{}^+$ which become chains.

The theoretical results for the charged ions should correspond most closely to the experimental conditions under which the charged species are produced directly, without secondary photoionization (spectra labeled $C_n{}^+$ and $C_n{}^-$ in Fig. 1).
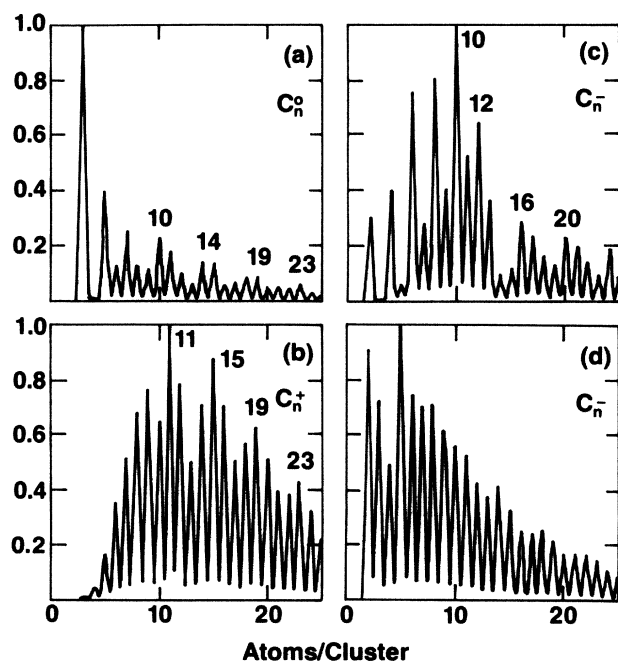
For the positive ions, the agreement is excellent for the larger ions (rings), where the magic numbers at 11, 15, 19, and 23 are well reproduced, as are the relative abundances for clusters between the magic numbers. For the smaller ions (chains) which are grown in the initial stages of cluster formation, there are large differences between the different experimental results [cf. Figs. 1(a)–1(c)]. These results seem to depend explicitly on the particular experimental conditions, including detectability and the kinetics of preparation at the initial stages of growth (e.g., the presence and strength of a shock wave).

For the negative ions, the overall shape of the spectrum for the larger clusters is well reproduced as are the magic numbers at 10, 12, and 16. The remaining discrepancies may be partially due to the approximations inherent in the MNDO method and in the simple approximation to the transition-state energies used in the present work. The negative-ion case is more sensitive, since the electron transfer process [cf. Eq. (8)] plays a major role in determining the relative cluster distribution. The negative-ion spectrum calculated without allowing for the charge-transfer terms [Fig. 3(d)] is significantly smoother and differs strongly from the experimental results. Thus the peak positions of negative ions depend both on the concentrations of clusters of a given mass and on their affinity. The $C_{10}{}^-$ peak stands out because both the relative stability [cf. Fig. 3(c)] and the electron affinity are high.

Finally, we turn to the neutral clusters. The theoretical cluster distribution [Fig. 3(a)] should correspond to the experimental spectra labeled $C_n \rightarrow C_n{}^+$ before photoionization. From a comparison between the experimental and theoretical results it is clear that the cluster distribution is strongly affected by the photoionization process. One effect is the size dependence of the photoionization threshold and cross section, which is not included in the calculations. For example, the photoionization thresholds of $4n + 3$ clusters are lower than these of $4n + 2$ clusters, because the last pair of π electrons occupies an antibonding state. The main differences, however, are probably due to photofragmentation. Indeed, it has been suggested by one of us[24] that a number of $4n + 3$ clusters are likely to arise from photofragmentation of $4(n + 1) + 2$ clusters. Both effects lead to the same magic numbers for the larger photoionized clusters as for those produced directly in the nozzle.

In summary, we have developed a multicomponent kinetic model of cluster formation which uses as input calculated geometrical and electronic parameters. Electronic structure calculations and kinetic simulations were carried out for the neutral, positive, and negative C_1–C_{25} clusters.

In the C_{10}–C_{25} range, the results predict the occurrence of monocyclic rings as the stable magic clusters. The maximum stabilities are at 10, 14, 18, and 23 for neutral clusters, and at 11, 15, 19, and 23 for positive clusters. For negative clusters, the crossover to rings should occur at $C_{13}{}^-$. The negative-ion spectra, however, are more influenced by the electron affinities of the clusters than by their relative stability, at least until $C_{16}{}^-$. For even larger clusters the electron affinity is greater, which would inhibit the overall rate of charge transfer and make the relative cluster stability more important.

FIG. 3. Calculated relative abundances for (a) neutral clusters, (b) positively charged clusters, (c) negatively charged clusters, and (d) negatively charged clusters calculated without charge-transfer effects. See text.

The calculations presented here show quantitatively that the cluster distribution depends both on the relative thermodynamic stability of the clusters and on the kinetics of their growth. Both effects are important in determining the final distribution of cluster sizes. The success of the mean-field kinetic model introduced here suggests a relatively simple way of accounting for most of the kinetic effects during the cluster growth process.

Note added. Firm experimental evidence for a structural transition at $n = 10$ for C_n^+ has recently been obtained by Geusic *et al.*[25]

[1]O. Echt, K. Sattler, and E. Recknagel, Phys. Rev. Lett. **47**, 1121 (1981); M. M. Kappes, R. W. Kunz, and E. Schumacher, Chem. Phys. Lett. **91**, 413 (1982).

[2]T. G. Dietz, M. A. Duncan, D. E. Powers, and R. E. Smalley, J. Chem. Phys. **74**, 6511 (1981); V. E. Bondybey and J. H. English, *ibid.* **74**, 6978 (1981).

[3]E. A. Rohlfing, D. M. Cox, and A. Kaldor, J. Chem. Phys. **81**, 3322 (1984).

[4]L. A. Bloomfield, R. R. Freeman, W. L. Brown, Phys. Rev. Lett. **54**, 2246 (1985).

[5]J. C. Phillips, Chem. Rev. (to be published).

[6]W. D. Knight, K. Clemenger, W. A. de Heer, W. A. Saunders, M. Y. Chou, and M. L. Cohen, Phys. Rev. Lett. **52**, 2141 (1984); K. Clemenger, Phys. Rev. B **32**, 1359 (1985).

[7]J. C. Phillips, J. Non-Cryst. Solids **34**, 153 (1979); Phys. Status Solidi B **101**, 473 (1980).

[8]N. Fürstenau and F. Hillenkamp, Int. J. Mass Spectrom. Ion Processes **37**, 155 (1981).

[9]L. A. Bloomfield, M. E. Geusic, R. R. Freeman, and W. L. Brown, Chem. Phys. Lett. **121**, 33 (1985).

[10]L. A. Bloomfield, R. R. Freeman, and W. L. Brown (unpublished).

[11]J. C. Phillips, J. Chem. Phys. **83**, 3330 (1985).

[12]K. Raghavachari and V. Logovinsky (unpublished); D. Tomanek and M. Schlüter (unpublished).

[13]See, for example, R. T. Morrison and R. N. Boyd, *Organic Chemistry,* 3rd ed. (Allyn and Bacon, Boston, 1973), p. 328.

[14]K. S. Pitzer and E. Clementi, J. Am. Chem. Soc. **21**, 4477 (1959); S. J. Strickler and K. S. Pitzer, in *Molecular Orbitals in Chemistry,* edited by B. Pullman and P. O. Löwdin (Academic, New York, 1964), p. 281. See also R. Hoffmann, Tetrahedron **22**, 521 (1966).

[15]M. J. S. Dewar and W. Thiel, J. Am. Chem. Soc. **99**, 4899 (1977); Quantum Chemistry Program Exchange, program No. 371 (unpublished).

[16]The geometry optimization for the neutral species was carried out under the constraint of all C—C bonds being equal. This was necessary because of the known tendency of semiempirical calculations to predict alternating single and triple carbon-carbon bonds (see Ref. 15, and references therein). We found this unrealistically exaggerated tendency in some of our calculations for rings and for charged species and have decided to omit this effect. Some degree of bond alternation may, however, exist in these systems.

[17]See S. Chandrasekkar, Rev. Mod. Phys. **15**, 1 (1943).

[18]Since ionization potentials are much greater than electron affinities for small and medium-size clusters, charge-transfer processes between the neutral and the positively charged clusters are much less likely and were neglected.

[19]H. W. Kroto, J. R. Heath, S. C. O'Brien, R. F. Curl, and R. E. Smalley, Nature **318**, 162 (1985).

[20]Even if a highly ionized plasma is created by the laser pulse, Coulomb attraction between the electrons and the positive ions will lead to a very fast recombination, making the population of neutral atoms much larger than that of ions.

[21]A similar approximation is often used in catalysis, where it is called the Polanyi-Bronsted relation. See E. A. Moelwyn-Hughes, *Physical Chemistry* (Pergamon, New York, 1961), p. 1265. These reactions take place much closer to equilibrium, and the successful extrapolation to cluster aggregation is encouraging.

[22]J. W. Moore and R. G. Pearson, *Kinetics and Mechanism,* 3rd ed. (Wiley, New York, 1981), p. 240.

[23]In units in which the growth time is $t = 1$, the other parameters are $X_1(t = 0)\alpha = 4.5$, $\gamma = 0.02$, and $\xi = 0.1$.

[24]J. C. Phillips (unpublished).

[25]M. E. Geusic, T. J. McIlrath, M. F. Jarrold, L. A. Bloomfield, R. R. Freeman, and W. L. Brown (unpublished).